nature materials

SUPPLEMENTARY INFORMATION

DOI: 10.1038/NMAT3200

Second harmonic generation in silicon waveguides strained by silicon nitride

M. Cazzanelli,[1] F. Bianco,[1] E. Borga,[1] G. Pucker,[2] M. Ghulinyan,[2] E. Degoli,[3] E. Luppi,[4,7] V. Véniard,[4] S. Ossicini,[3] D. Modotto,[5] S. Wabnitz,[5] R. Pierobon,[6] L. Pavesi[1,*]

1 Nanoscience Laboratory, Department of Physics, University of Trento, via Sommarive 14, 38123 Povo (Trento) Italy,
2 Advanced Photonics & Photovoltaics Unit, Bruno Kessler Foundation, via Sommarive 18, 38123 Povo (Trento), Italy,
3 Istituto di Nanoscienze-CNR-S3 and Dipartimento di Scienze e Metodi dell'Ingegneria, Università di Modena e Reggio Emilia, via Amendola 2 Pad. Morselli, I-42122 Reggio Emilia, Italy,
4 Laboratoire des Solides Irradiés, Ecole Polytechnique, Route de Saclay, F-91128 Palaiseau, France and European Theoretical Spectroscopy Facility (ETSF),
5 Department of Information Engineering, University of Brescia, Via Branze 38, 25123 Brescia, Italy,
6 CIVEN, via delle Industrie 5, I-30175, Venezia Marghera, Italy,
7 present address: Department of Chemistry, University of California Berkeley, CA 94720 USA
* e-mail: pavesi@science.unitn.it

DOI: 10.1038/NMAT3200

Ab-Initio Method:

1) Strained bulk-silicon structures: relation between Unit Cell, Strain and Periodic Boundary Conditions.

All the strained bulk-silicon structures studied were obtained using the supercell method starting from a unit cell of 16 silicon atoms initially in their bulk centro-symmetric positions. We report in Fig. 1a the unit cell together with the corresponding lattice vectors $\mathbf{a}_1$, $\mathbf{a}_2$ and $\mathbf{a}_3$. The unit cell is translationally repeated in the whole space by applying the vector $\mathbf{R} = n_1\mathbf{a}_1 + n_2\mathbf{a}_2 + n_3\mathbf{a}_3$ which is a linear combination through the integers n_1, n_2 and n_3 of the lattice vectors. In Fig. 1b we show the repeated unit cell with a couple of cells for each direction.

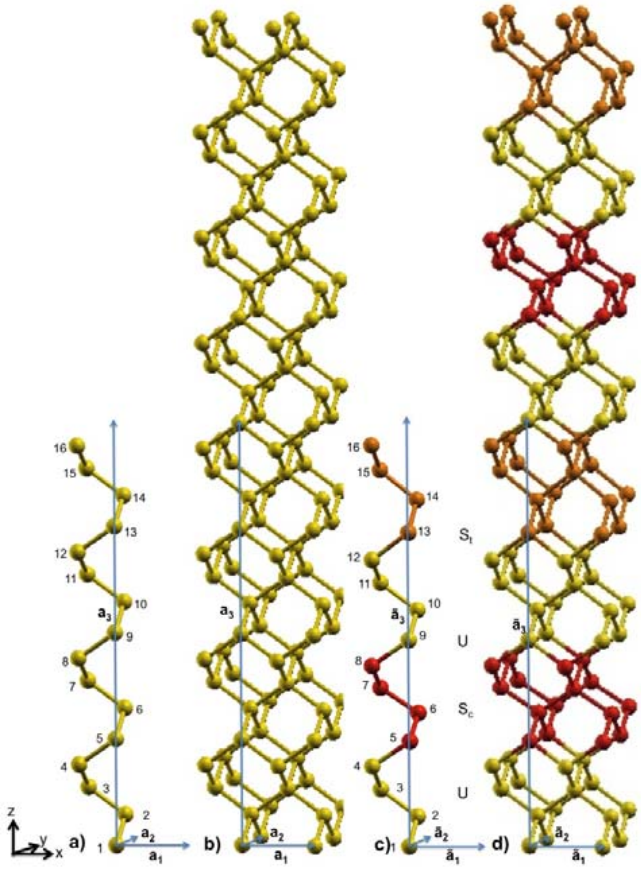

Figure 1. Unit cells of unstrained and strained bulk-Si structures
Fig. 1(a) Unit cell of 16 Si atoms for unstrained bulk and lattice vectors $\mathbf{a}_1$, $\mathbf{a}_2$ and $\mathbf{a}_3$. Atoms are labeled with a number from 1 to 16.
Fig. 1(b) Repeated unit cells (2 cells for each direction) as obtained from the application of lattice vectors $\mathbf{a}_1$, $\mathbf{a}_2$ and $\mathbf{a}_3$.
Fig. 1(c) Unit cell of 16 Si atoms for strained bulk (**US_tUS_c**/HY3 in the manuscript) and lattice vectors $\tilde{\mathbf{a}}_1$, $\tilde{\mathbf{a}}_2$ and $\tilde{\mathbf{a}}_3$. Atoms are labeled with a number from 1 to 16.
Fig. 1(d) Repeated unit cells (2 cells for each direction) as obtained from the application of lattice vectors $\tilde{\mathbf{a}}_1$, $\tilde{\mathbf{a}}_2$ and $\tilde{\mathbf{a}}_3$.
Yellow balls/sticks represents the unstrained silicon region, red balls/stick represents the compressive strained region and orange balls/sticks represents the tensile strain region.

In order to obtain the strained structures, we organized the 16 atoms in 4 groups of 4 atoms and we simulated strain by displacing Si atoms of just 2 of the 4 groups as shown in Fig. 1c. We labeled with **U** (yellow) the silicon atoms which were kept fixed at their bulk positions, while we labeled with **S** those silicon atoms which distances were modified in order to simulate a compressive $\mathbf{S_c}$ (red) and/or tensile $\mathbf{S_t}$ (orange) strain. In order to simulate continuous strain a crucial point is to choose the lattice vectors coherently with the applied strain as will be explained in details below. We had to re-define new lattice vectors $\tilde{\mathbf{a}}_1$, $\tilde{\mathbf{a}}_2$ and $\tilde{\mathbf{a}}_3$ for each of the strained structures and repeating the cell by the vector $\tilde{\mathbf{R}} = n_1\tilde{\mathbf{a}}_1 + n_2\tilde{\mathbf{a}}_2 + n_3\tilde{\mathbf{a}}_3$.
We applied a stress moving silicon atoms on the [110] plane along the (001) and (1,-1,0) directions and we identified two class of systems $\mathbf{US_tUS_t}$ and $\mathbf{US_cUS_t}$ (Fig. 2a and Fig. 3a). For each classes $\mathbf{US_cUS_t}$ and $\mathbf{US_tUS_t}$ we studied three structures in which we have progressively increased the applied strain. In Fig. 2b/c and Fig. 3b/c we show the maximum structural distortion in term of bond lengths and angles for $\mathbf{US_tUS_t}$ and $\mathbf{US_cUS_t}$ structures. The type and magnitude of strain is qualitatively observed as bond lengths and angles deviations with respect to the unstrained silicon bulk values.
To quantify the stress, each of the six structures have also been characterized by the stress tensor $\sigma_{i=X,Y,Z,j=X,Y,Z}$ and the pressure (HY) [1,2]. In fact, if we consider a volume element (unit cell) of our stressed structures, we can distinguish the effects of two types of forces: those acting directly in the interior of the element and those exerted upon the surface of the element by the surrounding material. The latter forces are related to the shear stress (SS) which corresponds to the off-diagonal elements of the stress tensor. In Tab. 1 and Tab. 2 we give the values of pressure (HY) and of the yz component of the SS (i.e. σ_{YZ}) for the $\mathbf{US_tUS_t}$ and $\mathbf{US_cUS_t}$ structures.

$\mathbf{US_tUS_t}$	HY (GPa)	SS (GPa)
HY1	1.71	$1.35\text{x}10^{-2}$
HY2	3.06	$6.71\text{x}10^{-2}$
HY3	3.06	$1.00\text{x}10^{-1}$

Table 1. Values of pressure (HY) and of the yz component of the SS (i.e. σ_{YZ}) for the $\mathbf{US_tUS_t}$ structures.

$\mathbf{US_cUS_t}$	HY (GPa)	SS (GPa)
HY1	0.32	$2.35\text{x}10^{-5}$
HY2	0.75	$2.19\text{x}10^{-3}$
HY3	0.91	0.12

Table 2. Values of pressure (HY) and of the yz component of the SS (i.e. σ_{YZ}) for the $\mathbf{US_cUS_t}$ structures.

We note that the magnitude of pressure and stress is always higher in $\mathbf{US_tUS_t}$ structures than in $\mathbf{US_cUS_t}$ ones. In fact, as the stress tensor is evaluated per unit-cell volume and it gives information about the global structure, in the case of $\mathbf{US_cUS_t}$, the compensation between tensile and compressive strain (different sign) result in lower HY and SS values. As a consequence the HY and σ_{YZ} are meaningful to compare structures only within the same class (i.e. $\mathbf{US_tUS_t}$ or $\mathbf{US_cUS_t}$).

DOI: 10.1038/NMAT3200

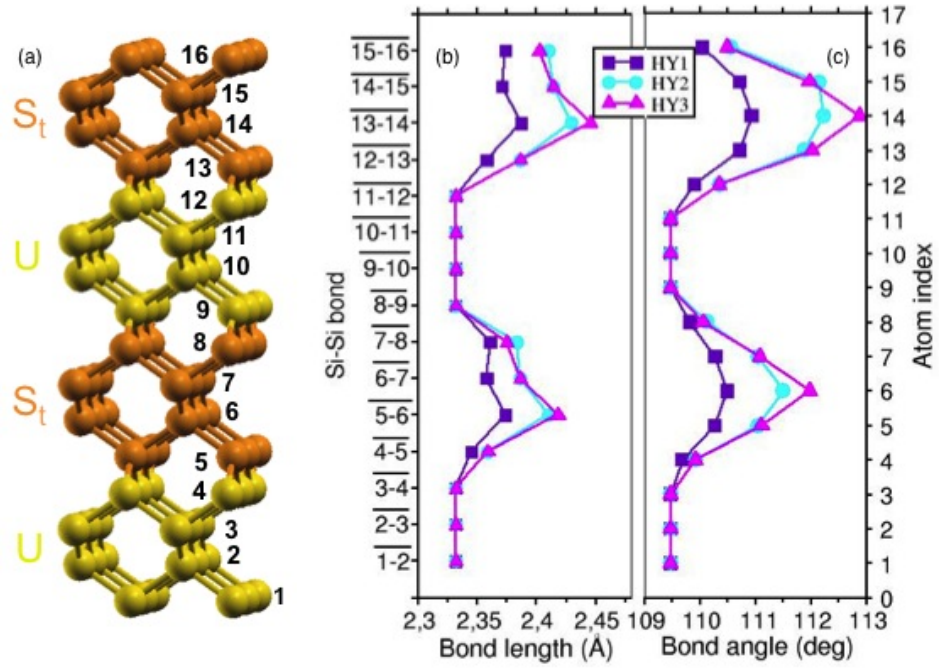

Figure 2. US_tUS_t structures.
Fig. 2(a) Simulation unit cell for **US_tUS_t** structures. Orange: bonds were elongated to represent a tensile stress. Yellow: no bond variations with respect to the relaxed silicon lattice (unperturbed region).
Fig. 2(b) Maximum bond length distortions for **US_tUS_t** structures. The unstrained bulk-Si bond lengths are 2.332 Å.
Fig. 2(c) Maximum bond angle distortions for **US_tUS_t** structures. The unstrained bulk-Si angles are 109.5°.

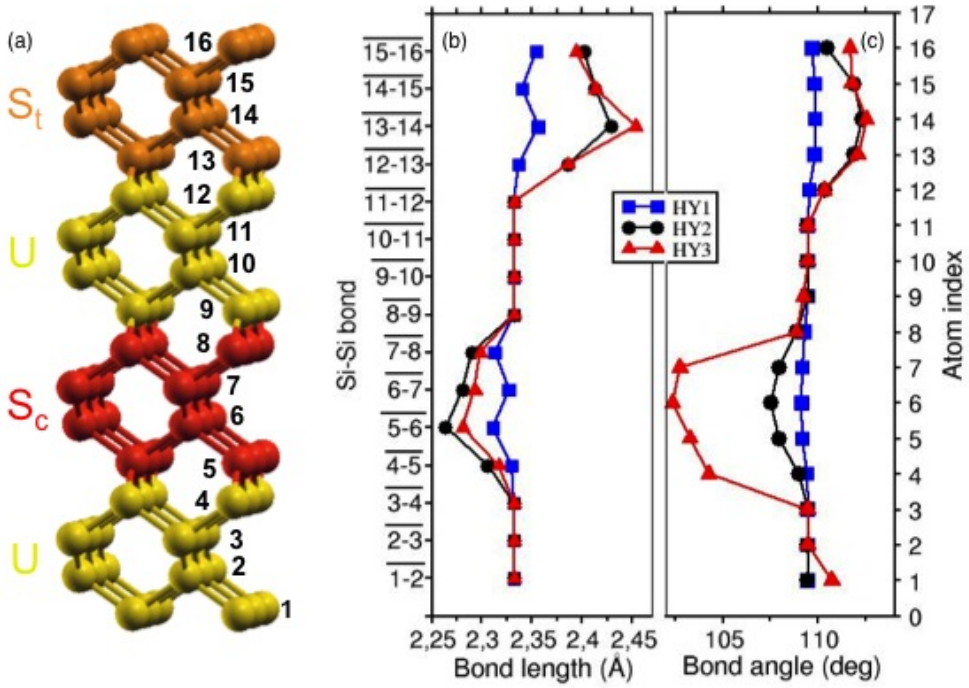

Fig. 3(a) Simulation unit cell for $\mathbf{US_cUS_t}$ structures. Orange: bonds were elongated to represent a tensile stress. Red: bonds were shortened to represent a compressive stress. Yellow: no bond variations with respect to the relaxed silicon lattice (unperturbed region).
Fig. 3(b) Maximum bond length distortions for $\mathbf{US_cUS_t}$ structures. The unstrained bulk-Si bond lengths are 2.333 Å.
Fig. 3(c) Maximum bond angle distortions for $\mathbf{US_cUS_t}$ structures. The unstrained bulk-Si angles are 109.5°.

Lattice vectors for the strained structures:

With our models we simulate continuous strain in a bulk system. A crucial point in the modeling of our structures is the way we have chosen the lattice vectors $\tilde{\mathbf{a}}_1$, $\tilde{\mathbf{a}}_2$ and $\tilde{\mathbf{a}}_3$. In fact, for each structure these vectors have to be properly and coherently chosen taking into account the applied strain as explained below.

We have chosen $\tilde{\mathbf{a}}_1=(\tilde{a}_1,0,0)$ equal to the lattice vector used for the unstrained bulk ($\mathbf{a}_1=(a_1,0,0)$) as no strain was applied in this direction. Also the vector $\tilde{\mathbf{a}}_2=(0,\tilde{a}_2,0)$ is unchanged with respect to the bulk ($\mathbf{a}_2=(0,a_2,0)$). In fact, as our unit cell is a chain of atoms the use of vector $\tilde{\mathbf{a}}_2= \mathbf{a}_2$ permits to periodically repeat in the Y direction the **U** (unstrained) regions without introducing any strain and also preserves the system from having strong additional strain at the $\mathbf{S_c}/\mathbf{S_t}$ (strained) regions.
In Fig. 4a/b we show the unstrained and strained silicon unit cell and their replica in Y direction through the vector $\tilde{\mathbf{R}}_1= 0\tilde{\mathbf{a}}_1 + 1\tilde{\mathbf{a}}_2 + 0\tilde{\mathbf{a}}_3 = (0,\ \tilde{a}_2\ ,0)$. The unstrained silicon unit cell is trivially repeated (Fig. 4a). For the strained unit cell (Fig. 4b) the **U** regions still continue to represent an unstrained bulk Si while in the repetition of $\mathbf{S_c}/\mathbf{S_t}$ the order of magnitude of strain at the border is the same as the one in the unit cell itself.
In particular, for $\mathbf{US_cUS_t}$/HY3 the strain ranges from 0.5% up to 5% while for all the other structures it ranges from 0.5% up to 3% compared to the bulk Si.
Instead, we modified $\tilde{\mathbf{a}}_3=(0,0,\tilde{a}_3)$ with respect to the unstrained bulk value. In fact, our unit cell is composed in the Z direction, of a compressive $\mathbf{S_c}$ and a tensile $\mathbf{S_t}$ regions which globally induce a change in the height of the cell along this direction. In the definition of $\tilde{\mathbf{a}}_3$ we take into account this height variation.
Moreover, we also impose a continuity condition between the replica which is explained through Fig. 5a/b. In this figure, we show the unstrained and strained silicon unit cell and its replica in Z direction through the vector $\tilde{\mathbf{R}}_2= 0\tilde{\mathbf{a}}_1 + 0\tilde{\mathbf{a}}_2 + 1\tilde{\mathbf{a}}_3 = (0,\ 0,\ \tilde{a}_3)$.
The continuity condition is to impose that the distance between atom 16 and 1b of the repeated structure is 2.332 Å (unstrained bulk distance). We find that, with respect to the angle of 109.5° in unstrained bulk silicon, these angles differ by ~1%-2% in this connecting region. With this criteria we did not add any strain defects at the edge of the cell between $\mathbf{S_t}$ and **U**.

DOI: 10.1038/NMAT3200

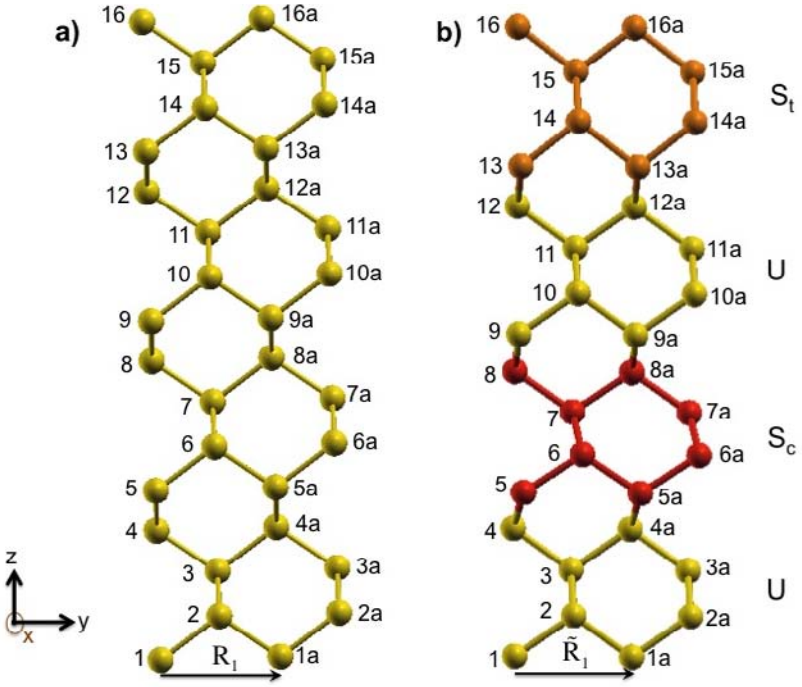

Figure 4. Unstrained and strained unit cell repetition in Y direction.
Fig. 4(a) Unit cell for unstrained bulk Si (1-16) and its repetition (1a-16a) through the vector $\mathbf{R}_1 = 0\mathbf{a}_1 + 1\mathbf{a}_2 + 0\mathbf{a}_3 = (0, a_2, 0)$.
Fig. 4(b) Unit cell for strained bulk Si (1-16) and its repetition (1a-16a) through the vector $\tilde{\mathbf{R}}_1 = 0\tilde{\mathbf{a}}_1 + 1\tilde{\mathbf{a}}_2 + 0\tilde{\mathbf{a}}_3 = (0, \tilde{a}_2, 0)$. The strained structure corresponds to $\mathbf{US_cUS_t}$/HY3.
Yellow balls/sticks represents the unstrained silicon region, red balls/stick represents the compressive strained region and orange balls/sticks represents the tensile strain region

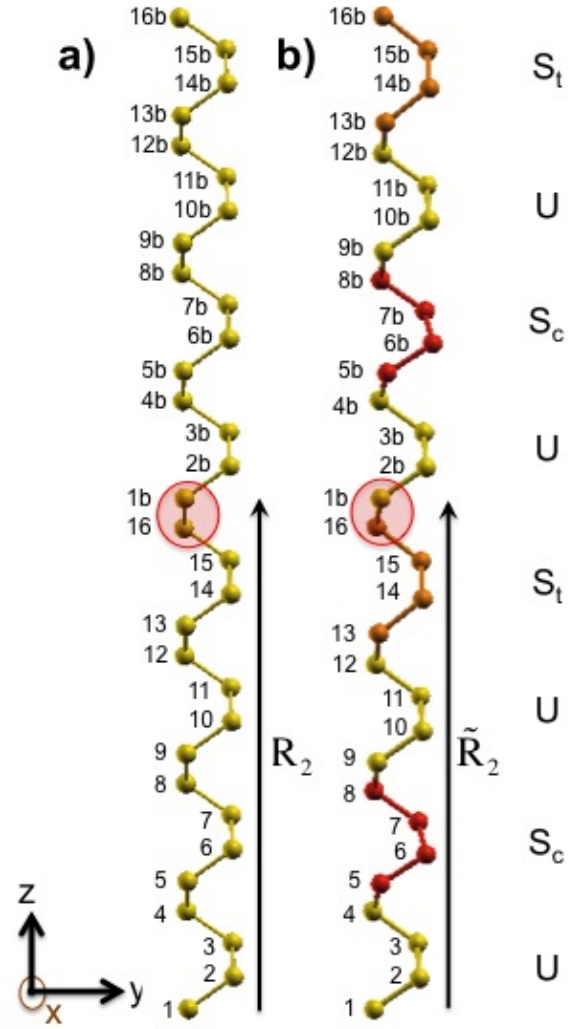

Figure 5. Unstrained and strained unit cell repetition in Z direction.
Fig. 5(a) Unit cell for unstrained bulk Si (1-16) and its repetition (1b-16b) through the vector $\mathbf{R}_2 = 0\mathbf{a}_1 + 0\mathbf{a}_2 + 1\mathbf{a}_3 = (0, 0, a_3)$.
Fig. 5(b) Unit cell for strained bulk Si (1-16) and its repetition (1b-16b) through the vector $\tilde{\mathbf{R}}_2 = 0\tilde{\mathbf{a}}_1 + 0\tilde{\mathbf{a}}_2 + 1\tilde{\mathbf{a}}_3 = (0, 0, \tilde{a}_3)$. The strained structure corresponds to $\mathbf{US_cUS_t}$/HY3.
Yellow balls/sticks represents the unstrained silicon region, red balls/stick represents the compressive strained region and orange balls/sticks represents the tensile strain region.

Below, we give the lattice vectors of all the structures presented:

Unstrained Bulk:	$\lvert\tilde{\mathbf{a}}_1\rvert$ = 3.808 Å, $\lvert\tilde{\mathbf{a}}_2\rvert$ = 3.808 Å, $\lvert\tilde{\mathbf{a}}_3\rvert$ = 21.544 Å.
$\mathbf{US_tUS_c}$/HY1:	$\lvert\tilde{\mathbf{a}}_1\rvert$ = 3.808 Å, $\lvert\tilde{\mathbf{a}}_2\rvert$ = 3.808 Å, $\lvert\tilde{\mathbf{a}}_3\rvert$ = 21.561 Å.
$\mathbf{US_tUS_c}$/HY2:	$\lvert\tilde{\mathbf{a}}_1\rvert$ = 3.808 Å, $\lvert\tilde{\mathbf{a}}_2\rvert$ = 3.808 Å, $\lvert\tilde{\mathbf{a}}_3\rvert$ = 21.726 Å.
$\mathbf{US_tUS_c}$/HY3:	$\lvert\tilde{\mathbf{a}}_1\rvert$ = 3.808 Å, $\lvert\tilde{\mathbf{a}}_2\rvert$ = 3.808 Å, $\lvert\tilde{\mathbf{a}}_3\rvert$ = 21.726 Å.
$\mathbf{US_tUS_t}$/HY1:	$\lvert\tilde{\mathbf{a}}_1\rvert$ = 3.808 Å, $\lvert\tilde{\mathbf{a}}_2\rvert$ = 3.808 Å, $\lvert\tilde{\mathbf{a}}_3\rvert$ = 21.896 Å.

DOI: 10.1038/NMAT3200

2) Calculation of $\chi^{(2)}$

We calculated the ground-state and electronic properties of strained bulk-silicon structures with the Density-Functional Theory (DFT). We used the local-density approximation (LDA), applying norm-conserving pseudopotentials [3] and plane-wave basis set with the ABINIT code [4]. In order to preserve the strain condition we did not relax our models. In fact, we verified that relaxing the systems brought them back into the initial unstrained ones.

We computed the second-order susceptibility $\chi^{(2)}$ and calculated the second-harmonic generation spectra for all the six strained bulk silicon structures. We obtained the nonlinear optical response using the *ab initio* formalism based on the Time-Dependent Density-Functional Theory (TDDFT) presented in Refs. [5] which has been implemented in the *2light* code [6,7].

$\chi^{(2)}$ was calculated in the Independent Particle Approximation and a scissor operator of 0.6 eV was used to simulate the quasiparticle energies [8]. The $\chi^{(2)}$ was obtained for light propagating in the direction (-1,1,0).

In Fig. 6(a/b/c) and Fig. 7(a/b/c) we show second-harmonic generation spectra for the structures $\mathbf{US_tUS_t}$ and $\mathbf{US_cUS_t}$ respectively. The general trend is that the magnitude of $\chi^{(2)}$ increases with the strain. Moreover, for an equal stress $\chi^{(2)}$ is higher in $\mathbf{US_cUS_t}$ than in $\mathbf{US_tUS_t}$: actually the $\mathbf{US_cUS_t}$ present stronger local inhomogeneity due to the change in the sign of the stress between the S_c and S_t regions. It is therefore possible, controlling the applied stress, to tune $\chi^{(2)}$ intensities in a very large range, from very few pm/V up to 200 pm/V.

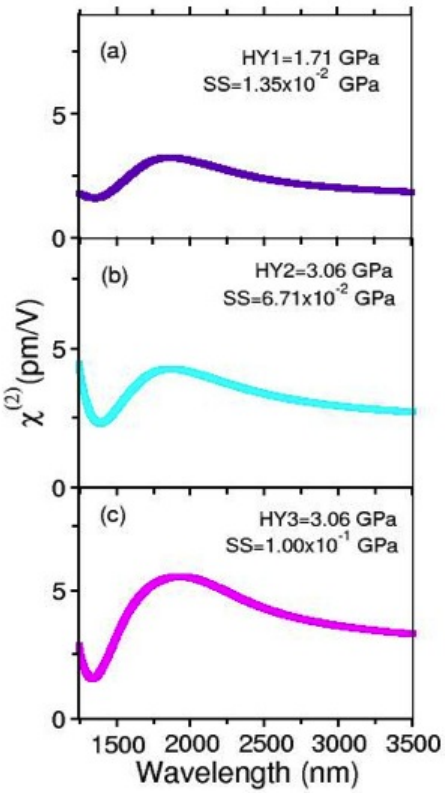

Fig. 6(a)-(c) Calculated $\chi^{(2)}$ for SHG spectra for the three structures of Fig. 2(b)-(c). The strain increases from the top to the bottom and manifests a progressive increase in the $\chi^{(2)}$ magnitude. The hierarchy of increasing strain in the three structures (violet-cyan-magenta) is reflected in the corresponding values of pressure (HY) and in the yz component of the Shear Stress (SS).

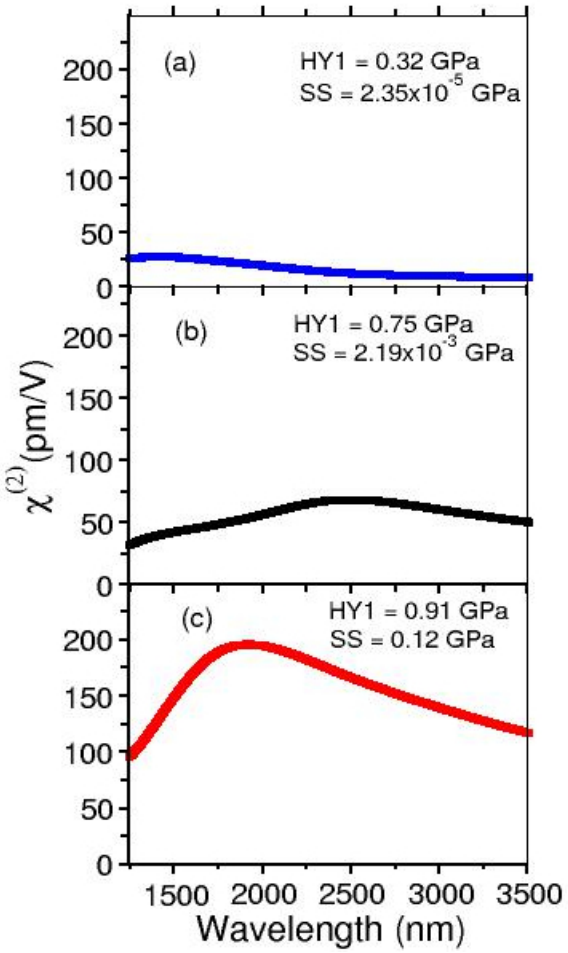

Figure 7. Simulated $\chi^{(2)}$ for SHG spectroscopy in US_cUS_t structures.
Fig. 7(a)-(c) Calculated $\chi^{(2)}$ for SHG spectra for the three structures of Fig. 3(b)-(c). The strain increases from the top to the bottom and manifests a progressive increase of the $\chi^{(2)}$ magnitude. The hierarchy of increasing strain in the three structures (blue-black-red) is reflected in the corresponding values of pressure (HY) and in the yz component of the Shear Stress (SS).

Interface effect on $\chi^{(2)}$: the example of Si/SiO_2

We investigated the role played by interface region supposing unstrained silicon. In fact, with the help of a model system we can neglect the rearrangement of silicon atoms at the interface with another material due to the mismatch between their lattice parameters. Therefore, we calculated the pure interface contribution to $\chi^{(2)}$. We considered SiO_2 in the beta-cristobalite metastable phase as the interface material (see the inset of Fig.8). This phase of the silicon dioxide has a 6% mismatch in the lattice parameter with respect to Si obtained by growing the SiO_2 layer rotated of 45° with respect to Si [9,10]. At the interface a Si atom per unit cell has two dangling bonds, which we saturated by two hydrogen atoms (inset of Fig. 8) [9]. The SiO_2 is strongly stressed by the Si lattice parameter, while Si does not undergo any strain. In Fig. 3) we show the calculated

DOI: 10.1038/NMAT3200

second-harmonic generation spectrum for the Si/SiO_2 interface. Despite the huge stress, the $\chi^{(2)}$ signal is always below 0.5 pm/V in the region of interest. The spectrum is of the order of magnitude of the $\chi^{(2)}$ for bulk silicon strained only along (0,0,1). Instead, it is negligible (less then 1%) with respect to the magnitude obtained for strained $\mathbf{US_cUS_t}$ structures where silicon atoms were moved in the [110] plane (Fig. 7). As a consequence the bulk contribution is expected to be dominant with respect to the interface contribution.

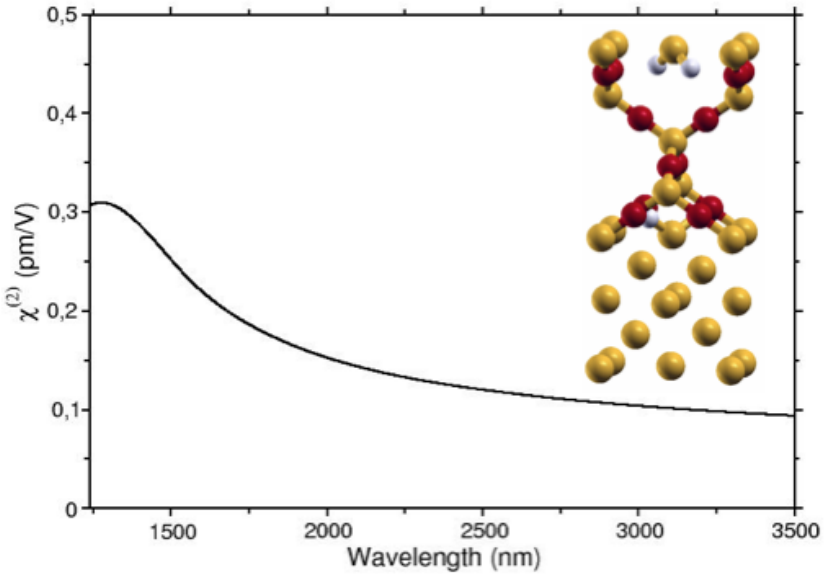

Figure 8. Calculated $\chi^{(2)}$ spectrum of the Si/SiO_2 interface.
In the inset the simulation unit cell: Si atoms (yellow balls), O atoms (red balls) and H atoms (white balls).

References

[1] Nielsen, O. H. & Martin, R. M. Quantum-mechanical theory of stress and force. *Phys. Rev. B* 32, 3780 (1985)
[2] Nielsen, O. H. & Martin, R. M. Stresses in semiconductors: Ab initio calculations on Si, Ge, and GaAs. *Phys. Rev. B* 32, 3792 (1985)
[3] Luppi, E., *et al* Accuracy of the pseudopotential approximation in *ab initio* theoretical spectroscopies. *Phys. Rev. B* **78**, 245124 (2008).
[4] Gonze, X. *et al*. ABINIT: First-principles approach to material and nanosystem properties. *Computer Phys. Commun.* **180**, 2582 (2009); Gonze, X. *et al.* A brief introduction to the ABINIT software package. *Zeit. Kristallogr.* **220**, 558 (2005).
[5] Luppi, E., Hübener, H. & Véniard, V. *Ab-initio* second-order nonlinear optics in solids. *J. Chem. Phys.* **132**, 241104 (2010).
[6] Luppi, E., Hübener, H. & Véniard, V. *Ab-initio* second-order nonlinear optics in solids: Second-harmonic generation spectroscopy from time-dependent density-functional theory. *Phys. Rev. B* **82**, 235201 (2010).
[7] Hübener, H., Luppi, E. & Véniard, V. *Ab initio* calculation of many-body effects on the second-harmonic generation spectra of hexagonal SiC polytypes. *Phys. Rev. B* **83**, 115205 (2011).
[8] Godby, R. W., Schluter, M. & Sham L. J. Self-energy operators and exchange-correlation potentials in semiconductors. *Phys. Rev. B* 37, 10159 (1988).
[9] Seino, K., Wagner, J.-M. & Bechstedt F. Ab initio calculation of optical absorption and reflectivity of $Si(001)/SiO_2$ superlattices with varying interfaces. *Appl. Surf. Sci*. 255, 787 (2008).
[10] Degoli, E. & Ossicini, The electronic and optical properties of Si/SiO_2 superlattices: role of confined and defect states. *Surf. Sci.* 32, 470 (2000).